Applied Mathematics and Mechanics (English Edition), 2007, **28**(11):1415–1426

Numerical simulation of flow in Hartmann resonance tube and flow in ultrasonic gas atomizer *

LI Bo (李博), HU Guo-hui (胡国辉), ZHOU Zhe-wei (周哲玮)

(Shanghai University, Shanghai Institute of Applied Mathematics and Mechanics, Shanghai 200072, P. R. China)

(Contributed by ZHOU Zhe-wei)

Abstract The gas flow in the Hartmann resonance tube is numerically investigated by the finite volume method based on the Roe solver. The oscillation of the flow is studied with the presence of a needle actuator set along the nozzle axis. Numerical results agree well with the theoretical and experimental results available. Numerical results indicate that the resonance mode of the resonance tube will switch by means of removing or adding the actuator. The gas flow in the ultrasonic gas atomization (USGA) nozzle is also studied by the same numerical methods. Oscillation caused by the Hartmann resonance tube structure, coupled with a secondary resonator, in the USGA nozzle is investigated. Effects of the variation of parameters on the oscillation are studied. The mechanism of the transition of subsonic flow to supersonic flow in the USGA nozzle is also discussed based on numerical results.

Key words Hartmann resonance tube, spray atomization, ultrasonic gas atomization, finite volume method, roe solver

Chinese Library Classification O354.2
2000 Mathematics Subject Classification 76N25
Digital Object Identifier(DOI) 10.1007/s10483-007-1101-6

Introduction

The Hartmann resonance tube is a device to generate high frequency oscillation in flow field. A typical Hartmann resonance tube consists of a cylindrical tube with a close end facing a high speed jet. High frequency oscillation will be generated. This device was invented by Hartmann[1] in 1919.

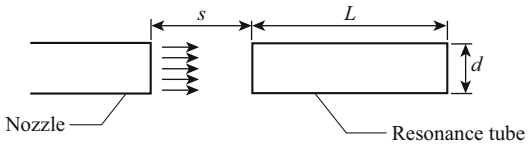

Fig. 1 Schematic diagram of Hartmann resonance tube

It was supposed that the oscillation in the Hartmann resonance tube can only occur when the jet is supersonic. Brocher, et al.[2] stated that if a thin needle was located along the nozzle axis as an actuator, oscillation would still occur even if the jet was subsonic. The actuator also helped to increase the intensity of oscillation and steadily maintained the oscillation. Brocher, et al.[2] explained that the total pressure of the jet was decreased in its center because of the

* Received Aug. 27, 2007; Revised Sep. 17, 2007
Corresponding author ZHOU Zhe-wei, Professor, E-mail: zhwzhou@shu.edu.cn

presence of the actuator, so that the outflow phase of the cycle will went more smoothly. The oscillation then reached to a "limit cycle". In the limit cycle, the amplitude can be steadily maintained. The oscillation frequency was given by linear acoustic theory,

$$f = \frac{c}{4L}, \tag{1}$$

where c is the local sound speed, L is the length of the resonance tube.

Sarohia and Back[3] discovered three resonance mode of the Hartmann Resonance tube: the jet instability mode, the jet regurgitant mode and the jet screech mode. Among them, the jet regurgitant mode has the highest amplitude and rather high frequency, so, the jet regurgitant mode is usually more preferred in practical applications.

The numerical simulations of the flow in the Hartmann resonance tube have been carried out in recent years. Hamed, et al.[4] numerically simulated the flow field of a HRT coupled with a needle actuator by the WIND code, and got computational results of the flow field in the jet regurgitant mode. The same authors later[5,6] studied an axisymmetric case by the WIND code, the effects of parameters and the distance between the nozzle exit and the tube mouth on the transition of resonance mode were discussed. Besides, Raman, et al.[7] numerically studied the flow in a high bandwidth resonance tube actuator by the WIND code, the pressure and velocity distributions are analyzed. Murugappan, et al.[8] simulated the resonance tube flow field by FLUENT software and compared the numerical results with experiments.

Spray atomization is a process that a liquid jet is impinged by high speed gas and breaks up into small droplets. As a basic physical process, it has been widely applied in powder metallurgy and spray forming technology. Grant[9] first introduced the ultrasonic gas atomization (USGA) nozzle into spray atomization. The configuration of the nozzle is shown in Fig. 2.

Former research indicated that in the USGA nozzle, when the nozzle inflow is steady, the outflow will become pulsating. Moreover, when the inflow is subsonic, the outflow can still be supersonic. The supersonic pulsating air jet will act positively on the atomization. The pressure oscillation of the gas jet is brought into the liquid metal jet by receptivity, which results in smaller size and finer distribution of the droplet size. Zhou and Tang[10] pointed out that this phenomenon is a result of the parametric resonance effect between the gas jet and the liquid metal jet. Simultaneously, since the droplet size decreases with the increase of the gas speed, the supersonic gas jet helps to thin the droplets after the break up. With all the effects mentioned above, the USGA nozzle effectively improves the product quality of spray forming.

The reason for the occurrence of the pulsating gas jet in the USGA nozzle is the effect of the Hartmann resonance tube structure in the nozzle. It is shown in Fig. 2 that the USGA nozzle consists of a Hartmann resonance tube coupled with a secondary resonator. Hence, in order to study the mechanism of the jet oscillation in the USGA nozzle, it is necessary to investigate the oscillation phenomenon in a basic Hartmann resonance tube.

Veistinen, et al.[11] gave the following explanation to the mechanism of the supersonic jet in the USGA nozzle: when the gas jet passes the outflow duct, affected by the thickening of the boundary layer near the crossing of the nozzle, the section of the jet will first reduce, then expand subsequently. The flow structure of this area appears like a converging-diverging Laval nozzle, see Fig. 3. The location of the minimum section area is called the "self-adjusting throat". At the self-adjusting throat, the gas flow changes from subsonic jet to supersonic jet. However, this explanation remains as an assumption until now and has not been proved by either experimental or numerical results.

Mansour, et al.[12] numerically simulated the flow in the USGA nozzle assuming the flow was steady. The flow structure inside the nozzle and downstream outside the nozzle is studied.

In this paper, The finite volume method based on the Roe solver of the Riemann problem is used to simulate the flow in the Hartmann resonance tube under the jet regurgitant mode with the presence of an actuator similar to Brocher's experiment[2]. The occurrence of oscillation and

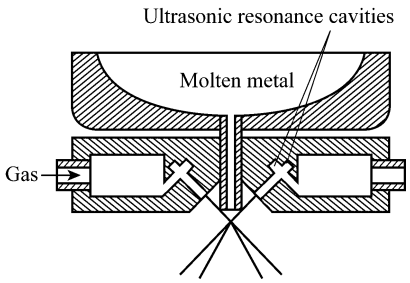

Fig. 2 Configuration of the USGA nozzle

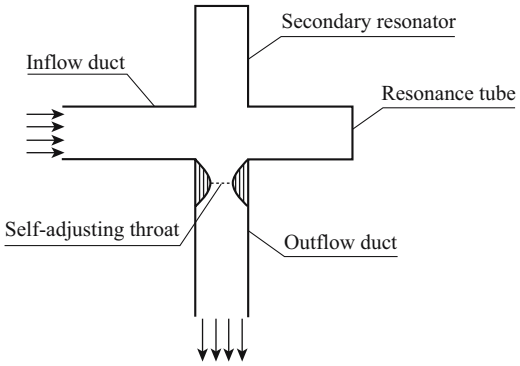

Fig. 3 Concepts of the resonance tube structure and the self-adjusting throat in the USGA nozzle

the factors affecting the oscillation are discussed; the computational results are compared with theoretical and experimental results available. The influences of the actuator on the transition of the resonance mode are further investigated.

The flow in the USGA nozzle is also simulated by the same numerical method. The jet oscillation caused by the Hartmann resonance tube structure in the nozzle and the transition mechanism of the jet from subsonic to supersonic are studied based on numerical results.

1 Methodology

A 2-D numerical model is set up. 2-D unsteady N-S equations in conservative form can be treated as the Euler equations plus the source terms:

$$\boldsymbol{U}_t + \boldsymbol{f}(\boldsymbol{U})_x + \boldsymbol{g}(\boldsymbol{U})_y = \boldsymbol{S}, \tag{2}$$

where

$$\boldsymbol{U} = \begin{pmatrix} \rho \\ \rho u \\ \rho v \\ e \end{pmatrix}, \quad \boldsymbol{f} = \begin{pmatrix} \rho u \\ \rho u^2 + p \\ \rho uv \\ u(e+p) \end{pmatrix}, \quad \boldsymbol{g} = \begin{pmatrix} \rho v \\ \rho vu \\ \rho v^2 + p \\ v(e+p) \end{pmatrix}, \quad \boldsymbol{S} = \begin{pmatrix} 0 \\ \mu\nabla^2 u \\ \mu\nabla^2 v \\ 0 \end{pmatrix}. \tag{3}$$

Here ρ is density; u and v are the velocities in x- and y-direction, respectively; e is the total energy of gas per volume unit; p is the gas pressure; and μ is the viscosity coefficient. The numerical Roe scheme[13] for 2-D Euler equations is

$$\boldsymbol{U}_{ij}^{n+1} = \boldsymbol{U}_{ij}^{n} - \frac{\Delta t}{\Delta x}\left(\tilde{\boldsymbol{f}}_{i+\frac{1}{2},j} - \tilde{\boldsymbol{f}}_{i-\frac{1}{2},j}\right) - \frac{\Delta t}{\Delta y}\left(\tilde{\boldsymbol{g}}_{i,j+\frac{1}{2}} - \tilde{\boldsymbol{g}}_{i,j-\frac{1}{2}}\right), \tag{4}$$

where $\tilde{\boldsymbol{f}}$ and $\tilde{\boldsymbol{g}}$ are the numerical flux of 2-D Euler equations constructed by the Roe method. For the N-S equations, first, let

$$\widehat{\boldsymbol{U}}_{ij}^{n+1} = \boldsymbol{U}_{ij}^{n} - \frac{\Delta t}{\Delta x}\left(\tilde{\boldsymbol{f}}_{i+\frac{1}{2},j} - \tilde{\boldsymbol{f}}_{i-\frac{1}{2},j}\right) - \frac{\Delta t}{\Delta y}\left(\tilde{\boldsymbol{g}}_{i,j+\frac{1}{2}} - \tilde{\boldsymbol{g}}_{i,j-\frac{1}{2}}\right). \tag{5}$$

Then,

$$\boldsymbol{U}_{ij}^{n+1} = \widehat{\boldsymbol{U}}_{ij}^{n+1} = \tilde{\boldsymbol{S}}_{ij}, \tag{6}$$

where $\tilde{\boldsymbol{S}}_{ij}$ is the numerical viscous term discretized by central differential method:

$$\tilde{\boldsymbol{S}}_{ij} = \begin{pmatrix} 0 \\ \mu\left[\frac{\Delta t}{\Delta x^2}(u_{i-1,j} - 2u_{i,j} + u_{i+1,j}) + \frac{\Delta t}{\Delta y^2}(u_{i,j-1} - 2u_{i,j} + u_{i,j+1})\right] \\ \mu\left[\frac{\Delta t}{\Delta x^2}(v_{i-1,j} - 2v_{i,j} + v_{i+1,j}) + \frac{\Delta t}{\Delta y^2}(v_{i,j-1} - 2v_{i,j} + v_{i,j+1})\right] \\ 0 \end{pmatrix}. \tag{7}$$

The computational domain of the Hartmann resonance tube flow field is divided into two sub-domains for computation. The domain of the USGA nozzle flow field is divided into four sub-domains, as shown in Fig. 4 and Fig. 5.

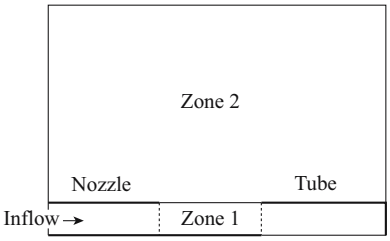

Fig. 4 Computational domains of the Hartmann resonance tube model

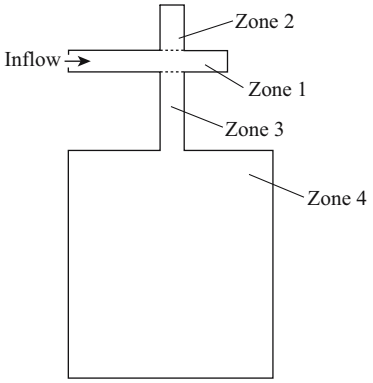

Fig. 5 Computational domains of the USGA nozzle model

2 Results and discussions

2.1 Computational results of flow field of Hartmann resonance tube

For a case of jet Mach number $Ma = 0.8$, tube diameter $d = 4.8$ cm, gap distance $s = 1.53d$, tube length $L = 1.8d$, the time step was set to be 8×10^{-8} s. After 250 000 time steps, the flow field shows obvious periodicity. The curve of net mass flux at the tube mouth vs. time step is shown in Fig. 6.

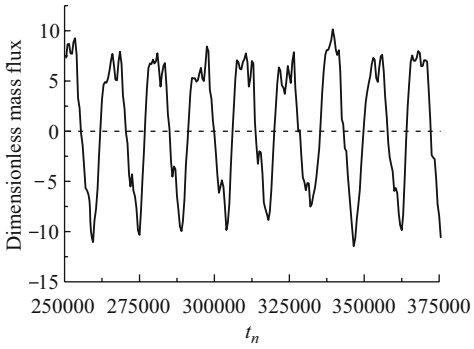

Fig. 6 Net mass flux fluctuation at the tube mouth

It can be observed from Fig. 6 that the mass flux at the tube mouth varies periodically with time. The flux-time curve fluctuates around zero, which means the periodical alternation

of inflow phase and outflow phase. The Hartmann resonance tube now operates in the jet regurgitant mode. The pressure-time at the tube end wall is shown in Fig. 7. It can be seen that the pressure oscillates periodically with time. The corresponding pressure spectrum figure is shown in Fig. 8. The peak frequency in the spectrum is measured to be 854 Hz, which is close to the theoretical frequency 955 Hz calculated by Eq. (1). The frequency of the same numerical model obtained by Hamed, et al.[4] by the WIND code, is 780 Hz. Comparatively, the result of present work is closer to the theory.

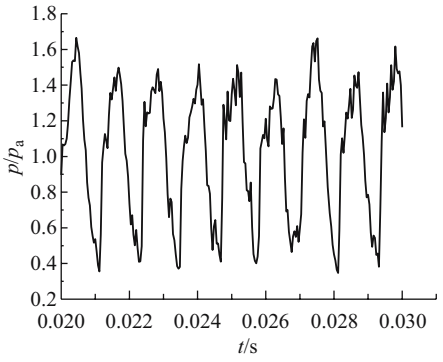

Fig. 7 Pressure oscillation at the tube end wall

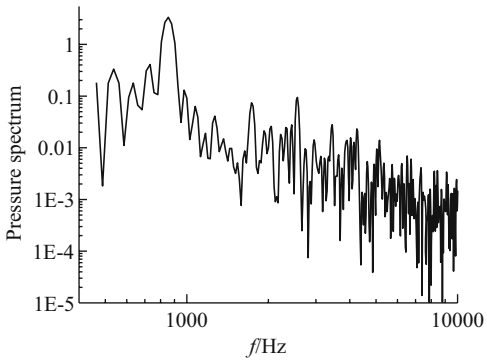

Fig. 8 Pressure spectrum at the tube end wall

The dimensionless pressure amplitude in Fig. 7 is $A = \Delta p/p_a = 0.984$, where p_a is atmospheric pressure. The amplitude, given by empirical equation[14], is

$$A = 2\gamma MaP_a, \tag{8}$$

which gives the amplitude $A = 1.615$. The computational amplitude is about 60% of the empirical counterpart. Considering the empirical formula is obtained ignoring some factors such as the viscous dissipation, and the amplitude observed in experiment was 60%∼80% of the empirical amplitude, the computational amplitude is quite reliable.

It can be concluded from Eq. (1) that the oscillation frequency depends only on the length of the tube and the sound speed, not on the jet Mach number. Therefore, the oscillation under the case of different tube length is investigated and the computational results are listed in Table 1.

It can be seen from Table 1 that the frequency goes down with the increase of tube length, which agrees well with the theory. At the same time, the amplitude goes up at first, and then goes down. The range of the amplitude variation is 29%, which indicates the amplitude does not vary too much.

Table 1 Frequencies and amplitudes of pressure oscillation at tube end wall with different tube lengths

L/d	Dimensionless amplitude A	Computational frequency f/Hz	Theoretical frequency f/Hz
0.6	0.789	1 294	2 865
0.8	0.850	1 196	2 148
1.0	0.962	1 148	1 719
1.2	1.059	1 025	1 432
1.5	1.105	928	1 146
1.8	0.984	854	955
2.0	0.851	708	859

The comparison of the computational frequencies and theoretical curve is shown in Fig. 9. When the tube is relatively long, the computational results agree well with the theory. However,

when the tube is relatively short, the computational frequencies are lower than the theoretical curve. The reason for this fact is that the buffering effect caused by the flow between the nozzle exit and the tube inlet is more significant for short tubes, which was also observed by former experimental research[7].

When the tube length is set to be $1.8d$, the other parameters are fixed, and the jet Mach number Ma is 0.6, 0.8 and 1.2, respectively, the flow field of the Hartmann resonance tube is investigated. The frequencies and amplitudes of pressure oscillation of the three cases are listed in Table 2. It can be concluded that the variation of Ma has no significant influence on the oscillation frequency, but mainly affects the amplitude A. A increases proportionally with the increase of Ma, which corresponds to Eq. (8).

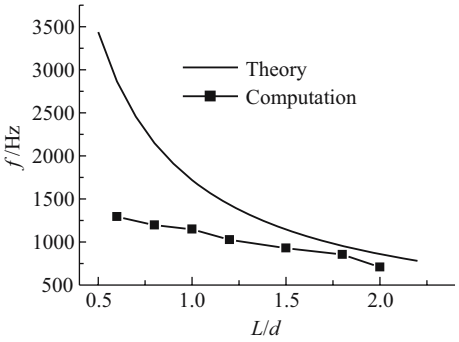

Fig. 9 Comparison of computational frequencies with theoretical curve

Table 2 Frequencies and amplitudes of pressure oscillation at tube end wall with different jet Mach numbers

Ma	f/Hz	A
0.6	831	0.782
0.8	854	0.984
1.2	903	1.626

The flow in the resonance tube with an actuator is studied above; next, the influences of the actuator on the flow will be further discussed. Brocher, et al[2] indicated that the presence of the actuator would reduce the total head around the axis of the flow coming out of the nozzle, which made the outflow phase to run more smoothly. The oscillation would then reach the "limit cycle". It was observed in experiments that if the actuator was removed from an oscillating flow field, the oscillation would immediately damp out. Brocher explained that this phenomenon was caused by the irreversible factors (such as viscous dissipation, shock wave, etc.) in the flow field. Next, the mechanism of the damping process will be discussed in detail based on the results of numerical simulation.

For a case of $Ma = 1.2$, $L = 1.8d$, with the presence of the actuator, from the results have been shown before, the flow field oscillates in the jet regurgitant mode with the periodical alternation of the inflow phase and the outflow phase. The oscillation frequency is 903 Hz. The dimensionless pressure amplitude at the axis of the tube end wall is 1.626.

After the computation of 625 000 time steps, the actuator is removed. During this process, the pressure-time curve at the axis of the tube end wall is shown in Fig. 10. It can be seen that the oscillation damps considerably, which agrees with the experimental result studied by Brocher, et al[2].

If the damping oscillation is due to the irreversible factors in the flow field, the oscillation amplitude should damp to zero and the flow becomes steady. However, it is observed that the oscillation does not damp out completely after removing the actuator, instead, the flow oscillates randomly at a rather small amplitude and high frequency, as shown in Fig. 11. The dimensionless pressure amplitude is 0.038, and the corresponding pressure spectrum (Fig. 12) shows no significant dominant frequency.

In order to study the flow structure, the velocity contour and pressure contour at time step $t_n = 750\,000$ are shown in Fig. 13 and Fig. 14.

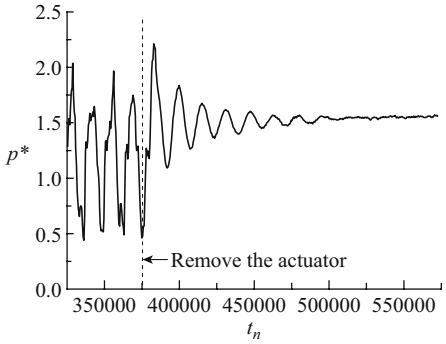

Fig. 10 Effect of removing actuator on pressure oscillation

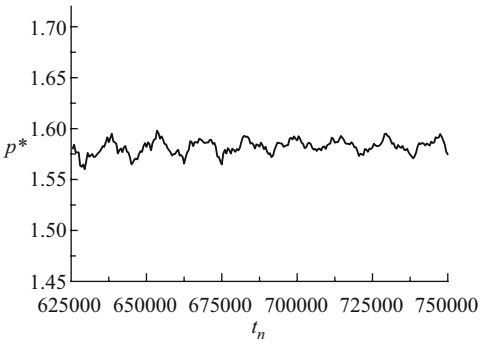

Fig. 11 Pressure oscillation in the jet screech mode

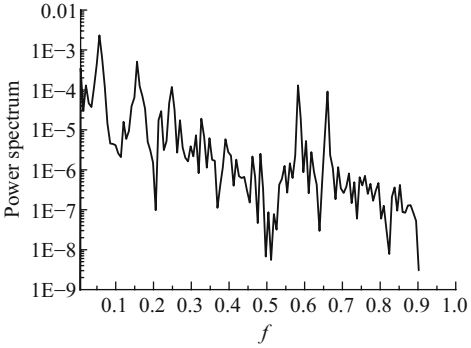

Fig. 12 Pressure spectrum in the jet screech mode

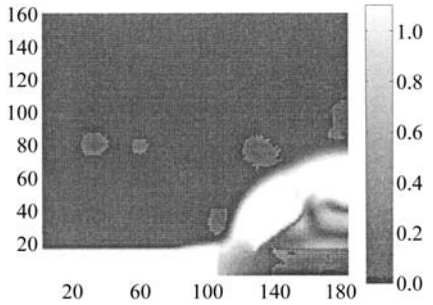

Fig. 13 Velocity contour at $t_n = 750\,000$

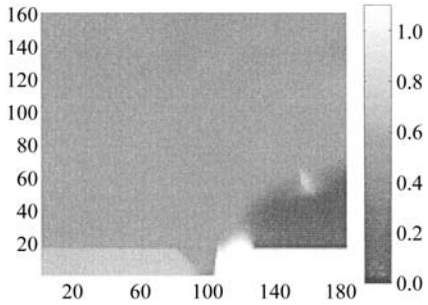

Fig. 14 Pressure contour at $t_n = 750\,000$

From the velocity contour, it can be observed that a shock wave appears at the gap between the nozzle exit and tube inlet, which makes the flow across the shock wave to decelerate from supersonic to subsonic. It can be seen from the pressure contour that after the jet passes the shock wave, its pressure increases sharply due to the effect of shock wave. A high pressure, high density and low speed region is formed from the shock wave to the tube inside. With the effects of this region, the jet after the shock wave is compressed and flows away above the tube inlet. The shock wave acts like a "lid" on the tube mouth.

The Mach number distribution in x-direction is shown in Fig. 15. The location of shock wave and the velocity jump at the shock wave can be clearly observed, which is very similar to the velocity distribution observed in Morch's experiment[15].

The occurrence of shock wave in front of the tube inlet and the change of the characteristics of pressure oscillation indicate that removing the actuator causes the resonance mode to switch from the jet regurgitant mode to the jet screech mode.

When the actuator is added again into the flow field in the jet screech mode, the shock wave structure at the tube mouth will be destroyed immediately. Periodical alternation of inflow phase and outflow phase and pressure oscillation will occur again, which means the adding of the actuator into the flow field in the jet screech mode will cause the resonance mode to switch from the jet screech mode to the jet regurgitant mode. The pressure-time curve during this process is shown in Fig. 16.

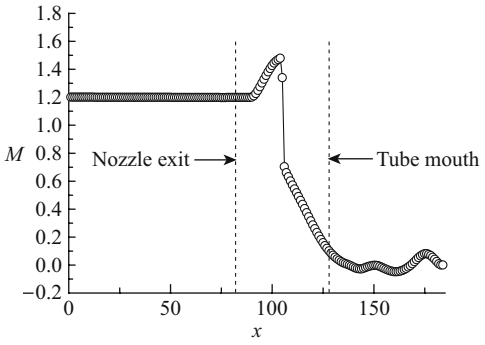

Fig. 15 Jet Mach number along the centerline at $t_n = 750\,000$

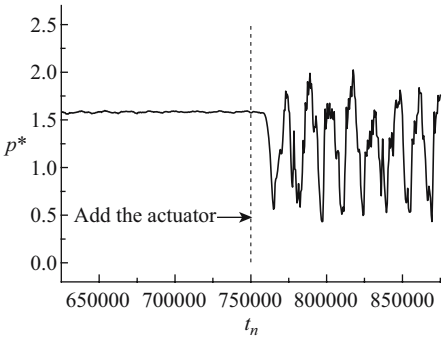

Fig. 16 Effect of adding the actuator on pressure oscillation

2.2 Computational results of the flow in the USGA nozzle

Considering a case that the jet Mach number is 0.8, the lengths of the resonance tube and the secondary resonator are equal to be 2 times of the tube diameter, that is, $L_1 = L_2 = 2d$. After the transient process, the flow field appears significant periodical characteristics. Each physical variable varies periodically with time. The flow at the nozzle exit is investigated, and the pressure-time curve and the corresponding spectrum are shown, respectively, in Fig. 17 and Fig. 18. The dimensionless frequency of pressure oscillation is 0.105 5, which is 12 060 Hz. From Eq. (1), for the parameters of this case, $f = 11\,910$ Hz. The computational frequency is quite close to the theoretical counterpart.

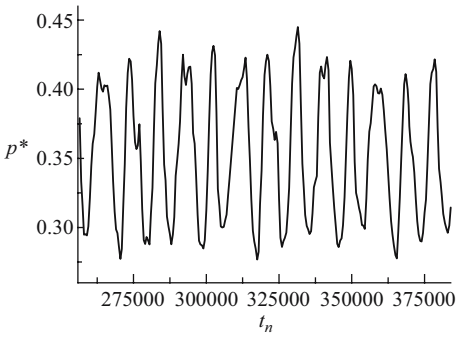

Fig. 17 Pressure oscillation at nozzle exit

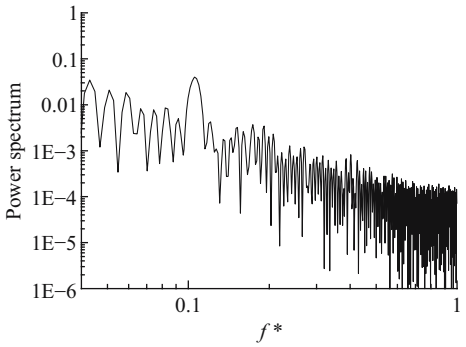

Fig. 18 Pressure spectrum at nozzle exit

The flux-time curves at the inlets of the resonance tube and the secondary resonator, respectively, are shown together in Fig. 19. Both the two curves fluctuate below and above zero, which means the periodical alternation of the inflow phase and the outflow phase happens at both the resonance tube and the secondary resonator. Therefore, the flow oscillation in the USGA nozzle is actually due to the cooperation of the simultaneous resonance in the jet regurgitant mode in the resonance tube and the secondary resonator. The generated oscillation will spread downstream.

Next, the effects of the change of the lengths of the resonance tube and the secondary resonator on oscillation are studied. When the lengths of the two tubes are equal to be $1d, 2d, 3d$ and $4d$, respectively, the calculated frequencies of the four cases are listed in Table 3.

It can be concluded that when the lengths of the resonance tube and the secondary resonator are equal, the increase of the tube lengths will cause the oscillation frequency to decrease. The frequency-tube length curve is shown in Fig. 20. As discussed above, both the resonance tube and the secondary resonator can be treated as a Hartmann resonance tube in the jet regurgitant mode, with the same oscillation frequency. Hence, the theoretical frequency-tube length curve of the jet regurgitant mode and the computational results are shown together in Fig. 20. It can be seen that the computational results agree very well with the theoretical curve.

For a configuration of $L_1 = L_2 = 2.0$, three cases of the jet Mach number Ma is, respectively, 0.7, 0.8 and 0.9 are calculated. The oscillation frequencies and amplitudes are listed in Table 4. It can be observed that the change of M does no significant effect on oscillation frequency, but mainly affects the amplitude. The amplitude increases with the increase of jet Mach number.

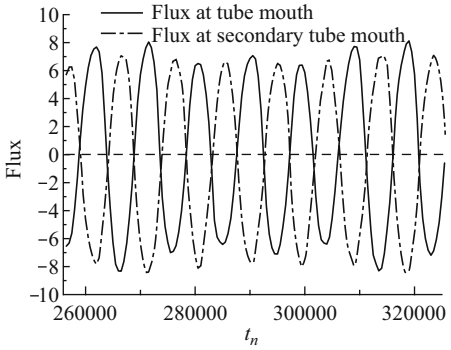

Fig. 19 Flux-time curves at the inlets of the resonance tube and the secondary resonator

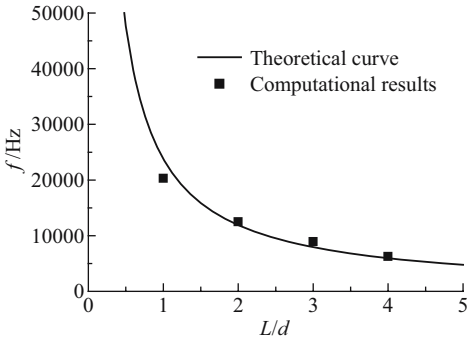

Fig. 20 Comparison of computational frequencies with theoretical curve

Table 3 Effects of geometric configurations on oscillation in the USGA nozzle

L_1	L_2	f/Hz
$1.0d$	$1.0d$	20 500
$2.0d$	$2.0d$	12 060
$3.0d$	$3.0d$	8 930
$4.0d$	$4.0d$	6 250

Table 4 Effects of jet Mach numbers on oscillation in the USGA nozzle

Ma	f^*	f/Hz	A
0.7	0.103 5	11 800	0.551
0.8	0.105 5	12 060	0.601
0.9	0.109 4	12 500	0.728

Besides generating pulsating jet, the USGA nozzle has another function of generating supersonic gas even if the inflow jet is subsonic. Veistinen[11], et al. supposed that the reason for this phenomenon is the existence of a "self-adusting throat" structure. When the jet passes this structure, its section area decreases at first, and then increases, as if passing a self-adjusting

Laval nozzle. The jet transits from subsonic to supersonic at the throat area.

Next, the existence of "self-adjusting throat" is investigated base on numerical results. For the case $Ma = 0.8, L_1 = L_2 = 2d$ as an example, the Mach number contour at a time after the occurrence of oscillation is shown in Fig. 21. It can be observed from the figure that when the jet passes the outflow duct, its section area reduces at first, and then increases, as if passing a Laval nozzle. The jet transits from subsonic to supersonic simultaneously, which correspond well with the "self-adjusting throat" assumption by Veistinen, et al[11].

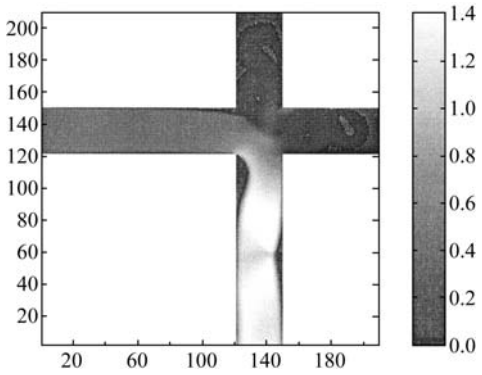

Fig. 21 Mach number contour of the flow in the USGA nozzle

The reason for the "self-adjusting throat" structure is that when the jet passes the corner of the outflow duct, affected by the geometric configuration and viscous boundary layer effects, some vortex structure is formed near the left wall of the outflow duct, so that the jet section area is reduced at that location. After the jet passes this area, its section area increases, so a throat structure similar to the Laval nozzle is formed. The flow vectors near at throat area are drawn in Fig. 22. Figure 23 is the contour of the throat area for $Ma = 1$. From Fig. 23 the shape and location of the critical line of the transition of the jet from subsonic to supersonic can be seen. Because the flow is two-dimensional, the critical line is not perpendicular to the tube wall, but a curve. It locates at the minimum section area of the flow. Near the two sidewalls, the velocity of the jet drop to zero due to the effects of viscous boundary layers.

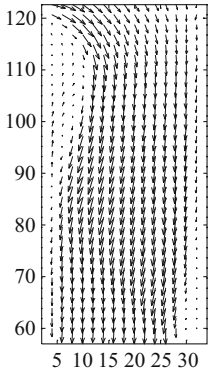

Fig. 22 Velocity vectors in the self-adjusting throat area

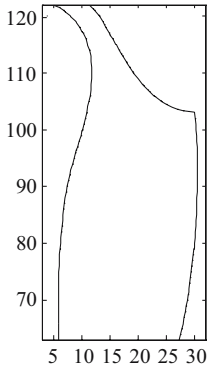

Fig. 23 Contour of the self-adjusting throat area for $Ma = 1$

3 Conclusions

The finite volume method based on the Roe solver to the Riemann problem is used to numerically simulate the flow in the Hartmann resonance tube. The oscillating flow field in the jet regurgitant mode, with the presence of an actuator is simulated. From numerical results, the initial transient flow can be observed. The oscillation occurs after the transient process. The periodical alternation of the inflow phase and outflow phase can be clearly identified. The frequency and amplitude of pressure oscillation agree well with theory. Effects of the variations of tube length and jet Mach number on the oscillation frequency amplitude are investigated. Numerical results indicate that tube length mainly affects the oscillation frequency, and jet Mach number mainly affects the oscillation amplitude. These tendencies agree well with theory. Influences of the actuator on the oscillation are further discussed. Numerical results show that if the actuator is removed from the flow in the jet regurgitant mode, the resonance mode will switch to the jet screech mode, and if the actuator is added into the flow in the jet screech mode, the resonance mode will switch back to the jet regurgitant mode.

The flow in the ultrasonic gas atomization nozzle (USGA nozzle) is numerically simulated by the same numerical method. Numerical results indicate that the oscillation occurs in the USGA nozzle. The oscillation results in the function of a Hartmann resonance tube structure coupled with a secondary resonator in the nozzle. The calculated oscillation frequency agrees well with theory. The tendency of the variation of the frequency with the lengths of the resonance tube and the secondary resonator agrees with the theory. The jet Mach number mainly affects the oscillation amplitude, and does not affect the frequency significantly. At the same time, there exists a "self-adjusting throat" structure inside the nozzle. The vortex structure near the sidewall of the outflow duct results in a reduction followed by expansion of the jet section area, similar to the Laval nozzle, where the jet transits from subsonic to supersonic. Numerical results correspond well with previous assumption of the mechanism of the supersonic jet.

References

[1] Hartmann J, Trolle B. A new acoustic generator[J]. *J Sci Instr*, 1927, **4**(4):101–111.

[2] Brocher E, Maresca A, Bournay M H. Fluid dynamics of the resonance tube[J]. *J Fluid Mech*, 1970, **43**(2):369–384.

[3] Sarohia V, Back L H. Experimental investigation of flow and heating in a resonance tube[J]. *J Fluid Mech*, 1979, **94**(4):649–672.

[4] Hamed A, Das K, Basu D. Numerical simulation of unsteady flow in resonance tube[R]. AIAA 2002-1118, 2002.

[5] Hamed A, Das K, Basu D. Numerical simulation and parametric study of Hartmann-sprenger tube based powered device[R]. AIAA-2003-0550, 2003.

[6] Hamed A, Das K, Basu D. Characterization of powered resonance tube for high frequency actuation[R]. FEDSM2003-45472, 2003.

[7] Raman G, Khanafseh S, Cain A B, Kerschen E. Development of high bandwidth powered resonance tube actuators with feedback control[J]. *Journal of Sound and Vibration*, 2004, **269**:1031–1062.

[8] Murugappan S, Gutmark E. Parametric study of the Hartmann-Sprenger tube[J]. *Experiments in Fluids*, 2005, **38**(6):813–823.

[9] Grant N J. Rapid solidification of metallic particulates[J]. *Journal of Metals*, 1983, **35**:20–26.

[10] Zhou Z W, Tang X D. The effect of the pulsation in gas flow on the stability of melted metal jet[C]. *Fourth International Conference on Spray Forming*, USA, 1999.

[11] Veistinen M K, Lavernia E J, Baram J C, Grant N J. Jet behavior in ultrasonic gas atomization[J]. *The International Journal of Powder Metallurgy*, 1989, **25**(2):89–92.

[12] Mansour A, Chigier N, Shih T, Kozarek R L. The effects of the Hartman cavity on the performance of the USGA nozzle needed for Aluminum spray forming[J]. *Atomization and Sprays*, 1998, **8**(1):1–24.

[13] Roe P L. Approximate Riemann solvers, parameter vectors, and difference schemes[J]. *Journal of Computational Physics*, 1981, **43**(2):357–372.

[14] Brocher E, Duport E. Resonance tubes in a subsonic flowfield[J]. *AIAA Journal*, 1988, **26**(5):548–552.

[15] Morch K A. A theory for the mode of operation of the Hartmann air jet generator[J]. *J Fluid Mech*, 1964, **20**(1):141–159.